Optimization of a portable nanoparticle detection device

Optimización de un dispositivo portátil de detección de nanopartículas

Oscar O. Soto-Rivera[1]

1   Licentiate degree in Electronic Engineering. Costa Rica Institute of Technology, School of Electronic Engineering, Costa Rica. Email: osotoriv@gmail.com

Tecnología en Marcha,
Vol. 33, especial Movilidad estudiantil. Octubre, 2020

188

Keywords

Abstract

The use of silver nanoparticles has grown in both the industrial and medical areas. Along its widespread use, interest in understanding its effects on the human body and the environment has also increased. As a result, novel and improved techniques and tools are being investigated to characterize this material. The neuroelectronics group at the Technical University of Munich is developing a portable device for detecting silver nanoparticles *in-situ*. To achieve this, using cell phone technology to communicate with the device is anticipated, as well as making the necessary calculations for the characterization of these nanoparticles. The system consists of analog and digital circuits which still require performance and portability optimizations, in such a way that they contribute to the successful completion of this task. This article will describe three phases for achieving device optimization. The first phase includes the design and implementation of a power management system, which will allow the portability of the sensor with an operating time of at least one hour. The second phase will be about noise characterization and reduction in the analog system. The third and last phase will focus on verifying the cutoff frequency of the circuit. In addition, this article will explain how these three phases relate to each other and contribute to optimizing the silver nanoparticle detection device.

Palabras clave

Resumen

El uso de nanopartículas de plata ha crecido tanto en el ámbito industrial como en el médico. Junto con su uso generalizado, también ha aumentado el interés por comprender sus efectos en el cuerpo humano y el medio ambiente. Como resultado, se están investigando técnicas y herramientas novedosas y mejoradas para caracterizar este material. El grupo de neuroelectrónica de la Universidad Técnica de Múnich está desarrollando un dispositivo portátil para detectar nanopartículas de plata in-situ. Para lograrlo, se prevé utilizar tecnología de telefonía celular para comunicarse con el dispositivo, así como realizar los cálculos necesarios para la caracterización de estas nanopartículas. El sistema consta de circuitos analógicos y digitales que aún requieren optimizaciones de rendimiento y portabilidad, de tal manera que contribuyan a la exitosa realización de esta tarea. Este artículo describirá tres fases para lograr la optimización del dispositivo. La primera fase incluye el diseño e implementación de un sistema de gestión de energía, que permitirá la portabilidad del sensor con un tiempo de funcionamiento de al menos una hora. La segunda fase tratara sobre la caracterización y reducción del ruido en el sistema analógico. La tercera y última fase se centrará en verificar la frecuencia de corte del circuito. Además, este artículo explicará cómo estas tres fases se relacionan entre sí y contribuirán a optimizar el dispositivo de detección de nanopartículas de plata.

Introduction

Due to the physical and chemical properties of silver nanoparticles, interest in their use has increased. Some of the products and industries using them include textiles, the automobile and electronics industry, health products, air and water treatment, among others [1-3]. This

has amplified human and environmental contact with these nanomaterials. However, the long-term effect of this interaction is not yet fully understood [2], [4]. As a result, interest has arisen in the study of silver nanoparticles and their effects, developing different techniques for their characterization. The device of this project uses the nano-impact technique based on the experiments carried out by Micka [5]. In this technique, an electrode is placed into the solution containing the nanoparticles and its potential is modified. When the nanoparticles interact with the electrode, a current spike on the order of picoamperes (pA) occurs. This electrical signal can be used to characterize the nanoparticles being studied [5].

In this project, the current spike is recorded by a device consisting of an analog and a digital system. The analog system has four circuits called PicoAmp which transform 1pA into 1mV, while the digital system converts an analog signal into a digital signal, store data and sends the information to a cell phone using a Bluetooth module. The cellphone runs an application that makes the necessary calculations to obtain useful data about the silver nanoparticles, such as their concentration or size. In order to create a portable silver nanoparticle detection device that uses the nano-impact method, enhancing the signal collection procedure is necessary. This process is linked to the physicochemical phenomenon happening in the electrode-nanoparticle interaction, as well as to the manipulation and reading of the current spike. Therefore, the characterization and reduction of electromagnetic noise in the system is a key factor to improve sensor's response and achieve adequate signal analysis. In addition, the device requires a power supply that meets its energy demand and at the same time provides portability. When designing the power supply, the noise this system adds to electronics shall be considered.

This work focuses on the characterization and reduction of noise in the analogue system, as well as on the verification of the cut-off frequency it was devised with. Jonathan N. Rapp was responsible for design and implementation, and it is based on a design built by Norbert Wolters at FZ Juelich [6]. The digital system was formulated by Handenur Çalışkan and implemented by Julian Feuerbach [7].

This article also describes the design and implementation process for a power management system that meets system power requirements, so that the sensor operates for at least one hour, while allowing portability to perform in-situ experiments.

This paper summarizes the most relevant work and results derived from an internship in the Neuroelectronics group of the Technical University of Munich. The information presented here is part of the work developed as a graduation project to obtain the Licentiate degree of Electronics Engineering [8].

First, some fundamentals of the nano-impact technique are briefly explained. Then, the design criteria that were used for the power management system are discussed. In addition, the scenarios and elements that were considered for the characterization and reduction of noise are described, as well as the methodology used for the verification of the cut-off frequency. Subsequently, the results achieved are presented and analyzed. Finally, the article presents the conclusions and recommendations obtained from this work.

Fundamentals

In the characterization of silver nanoparticles, two methods stand out: electron microscopy and optical methods [5], [9]. In electron microscopy, a difference can be made between the transmission electron microscope (TEM) and the scanning electron microscope (SEM) [5]. Regarding optical methods, there are light scattering techniques such as dynamic light scattering (DNS) and nanoparticle tracking analysis (NTA) [9]. Both, electron microscopy methods and light scattering techniques present some challenges when it comes to nanoparticles characterization.

Tecnología en Marcha,
Vol. 33, especial Movilidad estudiantil. Octubre, 2020

190

For example, the techniques used in electron microscopy are implemented out of the place where the sample was taken; sample preparation makes aggregation characterization difficult, and agglomeration does not provide kinetic information [5]. The main problem in light scattering techniques occurs when nanoparticles of different sizes coexist, since the result may be biased towards larger particles, thus delivering wrong conclusions [5]. Additionally, the methods described above are very expensive and require prior training and good handling of the equipment.

Nano impacts

As an alternative, the nano-impact electrochemistry technique is presented. Through this alternate, nanoparticles can be sized *in-situ*. To perform this technique, an electrode is introduced into a solution containing the silver nanoparticles being studied. The potential of the electrode can be modified. When some particle interacts with the electrode, a charge is released, the electrode absorbs it and causes a current spike in the pA range. This signal can then be used to obtain information on the size and concentration of silver nanoparticles [5]. Figure 1 shows the basic setup for conducting most nano-impact experiments. Here, there is a three electrodes configuration, the working electrode (WE) -which quantifies the electric power generated by the reaction-, a counter electrode (CE) and a reference electrode (RE), which helps to determine the potential difference at which the reaction between the working electrode and the nanoparticle occurs [5], [10]. The setup of the nanoparticle detection device being developed has two electrodes, specifically the working electrode and the reference electrode.
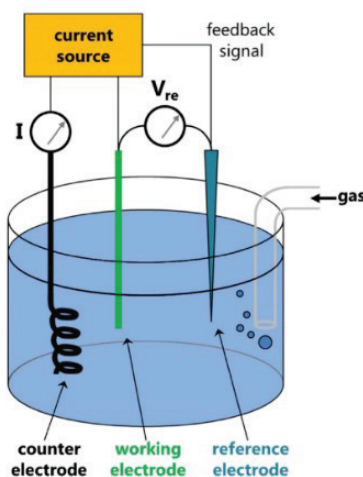
Figure 1. Three-electrode setup for nano-impact experiments. Source: [7].

When due to Brownian motion the nanoparticle approaches the working electrode, an oxidation reaction takes place because of the potential difference between this and the reference electrode. This reaction releases a charge from the nanoparticle which is then absorbed by the electronics through the working electrode. This charge produces a current spike that may be studied to obtain information related to the nanoparticle. For example, if a complete oxidation and a spherical shape are assumed, knowing the nanoparticle size is possible with the current spike integral. Furthermore, when there are multiple impacts by several nanoparticles, quantifying the number of current spikes can provide information about concentration [2], [5], [11].
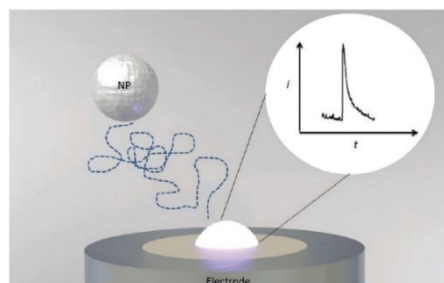
Figure 2. Illustration of nano impact and current spike generated by the oxidation
reaction between the nanoparticle and the working electrode. Source: [5].

The accuracy of this method is influenced by three main aspects: charge transfer characteristic, mass transport and the measurement system, which includes the electronics used. The noise in the electronic system must be lower than the signal to be measured in order to study it [5].

Cutoff frequency

Figure 3 exemplifies the current spike captured by the working electrode versus a single impact from a nanoparticle. The red trace corresponds to the impact of a 10 nm nanoparticle with a 3 μm electrode. The blue trace represents the impact of a 20 nm nanoparticle with a 24 μm electrode [9].
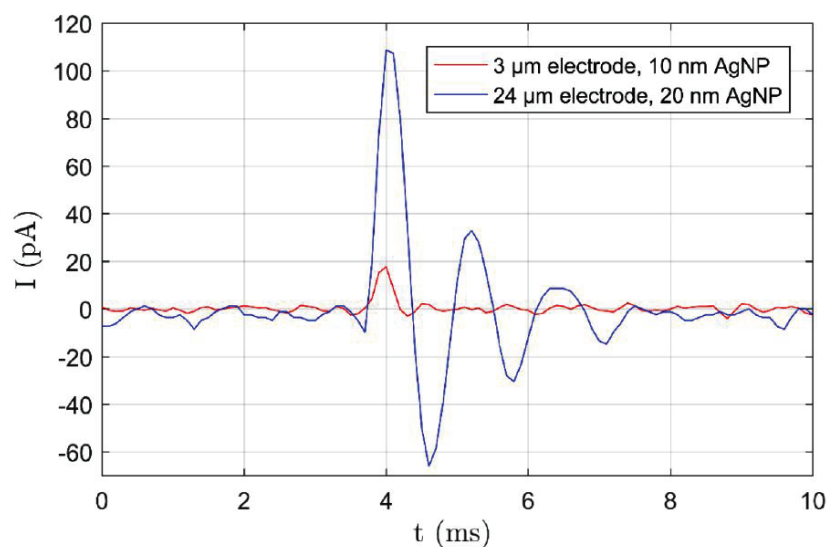
Figure 3. Current spike due to nano impacts. Source [9].

Useful information occurs in the first oscillation; the other oscillations derive from system electronics instabilities. To reduce these oscillations, a low-pass filter is used. Using this filter adds an additional benefit: the cutoff frequency allows modifying the length or width of the current spike. By changing signal length, amplitude varies too, preserving the area under the curve, which allows to continue obtaining the nanoparticle's size [12].
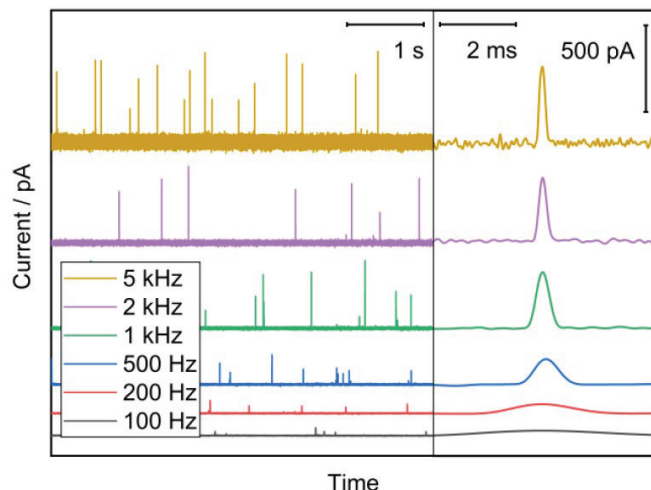
Figure 4. Change in the current spike when using different cutoff frequencies in the low-pass filter. Source: [12].

Concentration measurement depends on the diffusion coefficient provided by equation 1. The use of low cut-off frequencies may lead to incorrect results in this parameter as a result of increased length [12].

$$D_{x^-} = \frac{\rho r^2}{2\ln(2)N_A t_{dur} C_{x^-}} \qquad (1)$$

D_{x^-} is the diffusion coefficient for ion X^-; C_{x^-} is the concentration of the anion; ρ is density of nanoparticle and t_{dur} is the time of the transformative impact signal [12]. .

Noise

Usually, circuit noise is an unpredictable and unwanted signal that affects system performance. The term noise floor refers to the noise level at a circuit output in the absence of an input signal [13]. This defines the minimum signal that can be registered by the circuit. A lower noise floor makes the sensor more sensitive to smaller electrical signals, or in other words, it increases sensor's sensitivity.

Circuit noise originates in external and internal sources. Some internal sources of noise are the operational amplifiers (Op-Amps) or the PCB layout, while external noise sources may include nearby electronics, fluorescent lights, or the environment. With proper shielding, reducing the noise generated by external sources is possible in order to analyze only the noise from internal sources [13-16].

Materials and methods

Design and implementation of a power management system

The analog system has four channels, each with an identical PicoAmp circuit. In addition, circuit input allows coupling of a printed sensor made up of an array of microelectrodes. When the project started, the device was fed by a TENMA 72-10495 power source. This power source not only made portability difficult due to its size and weight, but it also added noise due to the power line, as will be shown later. To solve these difficulties, a power management system was designed and implemented. The design process began with establishing power requirements for both, the analog and digital circuits.
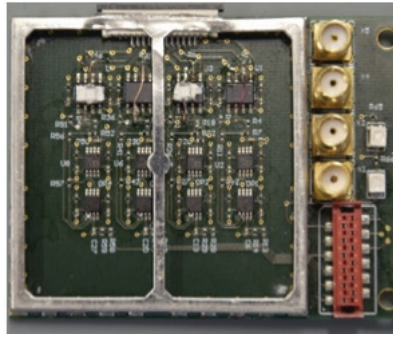
Figure 5. Four-channel analog circuit. Source [8].

Quiescent current was used [17] in order to get the maximum current necessary that the power system must provide for the analog system. This is the current flowing in an Op-Amp when its output is connected to a high impedance load. All the Op-Amp in the PicoAmp circuit have their output connected to the input of another Op-Amp, which is high impedance. Although this system has four PicoAmp circuits, an upcoming eight-channel design will be created. Therefore, the power system was designed with this future upgrade in mind. The maximum currents and voltages for the digital system were obtained from the datasheets of each component. Tables 1 and 2 summarize current and voltage requirements for both systems.

Table 1. Current and voltage requirements for the digital circuit. Source: [8].

Component	Model number	Quantity	Voltage supplied (V)	Maximum current supplied (mA)	Total maximum current supplied per component (mA)
ADC	ADS8688	1	+5	16	16
Voltage reference	REF5040	1	+5	1.2	1.2
DAC	DAC8563	1	+3.3	1.6	1.6
Voltage reference	REF2033	1	+5	0.46	0.46
Dual Op-Amp	OPA2188	1	+5	0.6	0.6
Bluetooth module	RN-42	1	+3.3	50	50
Voltage inverter	LM2776	1	+5	0.2	0.2
Microprocessor	STM32F429I	1	+3.3	46.8	46.8

Table 2. Current and voltage requirements for the analog circuit. Source: [8].

Component	Model number	Quantity	Voltage supplied (V)	Maximum current supplied (mA)	Total maximum current supplied per component (mA)
Ultra-Low input biased amplifier	OPA129UB	8	±5	1.8	14.4
Voltage offset amplifier	AD822A	8	±5	1.6	12.8
Summing amplifier	AD820A	8	±5	0.8	6.4

The sum of total maximum current supplied per component in tables 1 and 2 determines the maximum current that each voltage level or power rail must be capable of supplying. This information is summarized in table 3.

Table 3. Voltage and current required by digital and analog circuits. Source: [8].

Power rails voltage (V)	Current (mA)
+3.3	52.06
+5	33.6
-5	98.4

In order for the device to operate for at least one hour and meeting the requirements set out in table 3, a battery of at least 200 mAh is required. However, commercial batteries between 1800 mAh and 2000 mAh are available at affordable prices. These batteries increase the operating time of the device and meet power requirements. In addition, their compact size makes them ideal for portable devices.

Another consideration when designing the power management system is the noise that will be added to the overall system. Consequently, circuit design and its components should introduce the least amount of noise to the sensor. The general blocks for the proposed design are shown in figure 6, and table 4 details the components that were used for implementing the design.
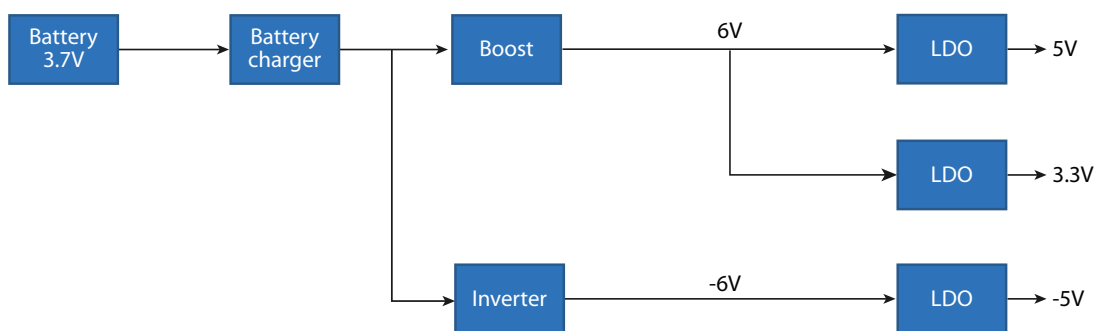
Figure 6. Block diagram of the power circuit.

Table 4. Components used in the power circuit. Source: [8].

Function	Component
Battery charger	BQ2506
Boost and Inverter circuits	TPS65131
LDO to generate + 5V and + 3.3V	TPS7A47
LDO to generate -5V	TPS7A33

The power circuit is fed by a LI-ION battery of 3.7 V as nominal voltage and with a 2050 mAh capacity. The charging circuit for this battery was included in the power management system.

The nominal battery voltage is within the voltage levels required for the nanoparticle device. As a consequence, voltage regulators must be used to reach the desired levels. Battery voltage was set to ± 6 V with Boost and Inverter circuits. Voltage levels in table 3 are generated with the help of Low-Dropout Regulators (LDO). Despite battery discharging over time, the Boost and

Inverter circuits keep a stable input voltage for the LDOs. As a result, supply voltage for the silver nanoparticle sensor also remains stable.

The Boost circuit is used when the desired output voltage is greater than the input voltage, while the inverter circuit is used when the desired output voltage has opposite polarity to the input voltage [18-20]. However, the Boost and inverter circuits produce noise due to the switching frequency of the transistor controlling output voltage, and this noise is added to the rest of the system [21].

LDOs not only help set the desired end voltage, but are ideal for filtering noise because of transistor switching of Boost and Inverter topologies. Furthermore, LDOs benefit from the output voltage of these topologies, since their input voltage shall be greater than output voltage [22], [23]. The chosen LDOs are ultra-low noise and thus, the amount of noise added to the sensor is minimized.

Circuit schematics and layout were made using the Altium Designer 18 software. The PCB design criteria set in the data sheets and application notes for each component were followed.

Characterization and noise reduction in the analog circuit

The Peak-to-Peak value (Pk-to-Pk), the Root Mean Square (RMS) and the Power Spectral Density (PSD) [23-25] were used to study the noise in the analogue system. These tools allow characterizing this random signal [26-28].

The conversion from 1 pA to 1 mV made by the PicoAmp circuit requires a feedback resistor. It was experimentally evaluated whether the position at which this resistor is connected to the Op-Amp has any effect on reducing noise in the circuit. Figure 7 illustrates the four resistors arrangement, one for each channel.
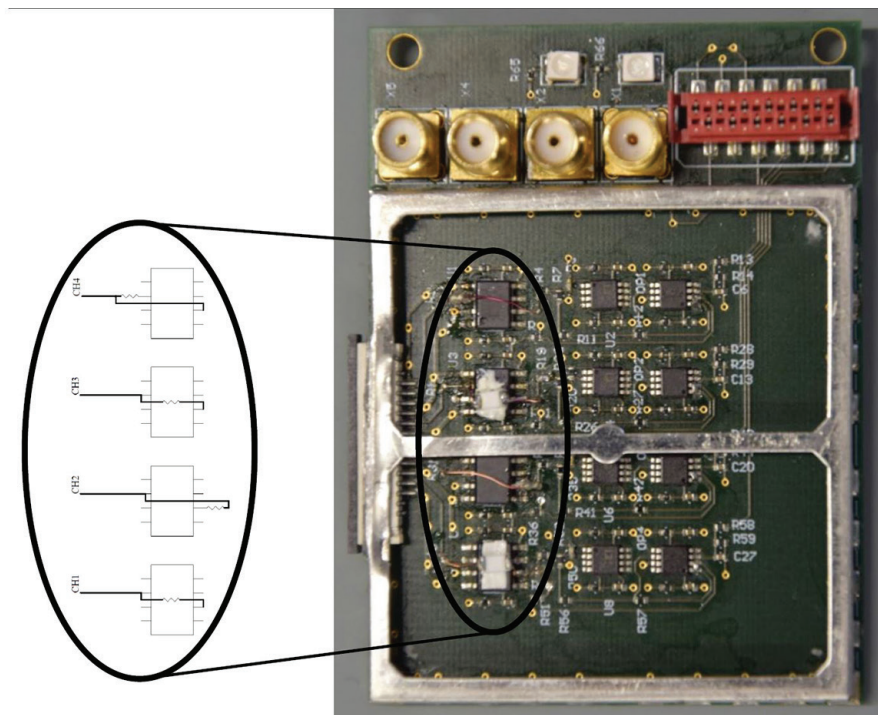
Figure 7. Feedback resistors in different positions. Source [8].

Tecnología en Marcha,
Vol. 33, especial Movilidad estudiantil. Octubre, 2020

196

At the moment of developing this project, channel 3 did not work. However, the position of the feedback resistor was the same as in channel 1, so its effect could still be evaluated.

Silver nanoparticles are detected by placing the electrolyte on a printed sensor coupled to the analog system's input. Through this sensor, the current spike is recorded by the PicoAmp circuit. The electrode-electrolyte interface and the antenna-like behavior of the printed sensor add noise to the system once it is coupled to it. The experiments and improvements carried out made it possible to quantify the noise level added by these factors.

Verification on the circuit cut-off frequency

The analog circuit was designed to interact with 50 nm silver nanoparticles and for the first oscillation shown in figure 3 to be 0.303 ms. To achieve this, the cutoff frequency of the low- pass filter was planned to be 3.3 KHz. Cutoff frequency was calculated using the ratio of the output signal to the input signal using a frequency sweep from 400 Hz to 12 KHz.

Results

Power management system

Figure 8 shows the final result of the PCB manufacturing for the power management system. A multimeter was used to measure output voltages as well as the maximum current delivered by the power rails. Output voltage results correspond to those in table 3. The total output current for the positive power rails is 400 mA, and -400 mA for the negative power rail. These results satisfactorily meet the power requirements of the silver nanoparticle detection device.
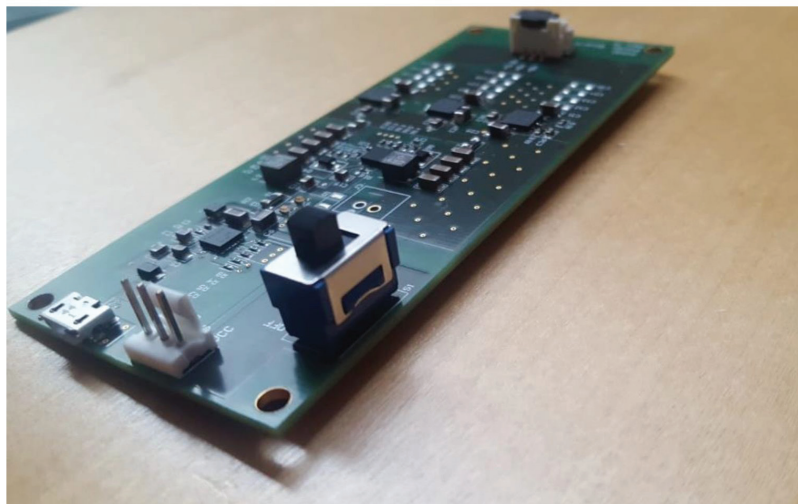
Figure 8. Power circuit PCB. Source [8].

To determine the operating time of the device when connected to this new power system, the LI-ION battery charge and discharge characteristic curve was used. This information was obtained with the help of the VSP-300 Bio-Logic Science Instruments. This equipment helped to set a constant load on the battery and thus, configure different current demands corresponding to diverse amounts of connected channels (PicoAmp circuits). Table 5 summarizes the three most relevant channel quantity settings for the device and their corresponding operating time.

Setting 1 represents the number of channels currently in use, setting 2 will be present for a future analog system upgrade and setting 3 determines the maximum number of channels that may be fed by the power management system. The initial goal was to operate the device for one hour; however, the new power source exceeds this goal by 10 hours and 30 minutes. In all cases, battery charging time is 3 hours and 50 minutes.

Table 5. Discharge time according to the number of channels. Source: [8].

Configuration	Number of channels	LI-ION battery discharge time
1	4	11 h and 30 min
2	8	9 h and 45 min
3	60	3 h and 45 min

To determine the load that should be connected to the battery, the current used by the digital circuit, the power circuit and the amount of current required by each channel in the analog system were added. Afterwards, the number of channels that may be added was determined so that the total current does not exceed 400 mA in any of the power rails.
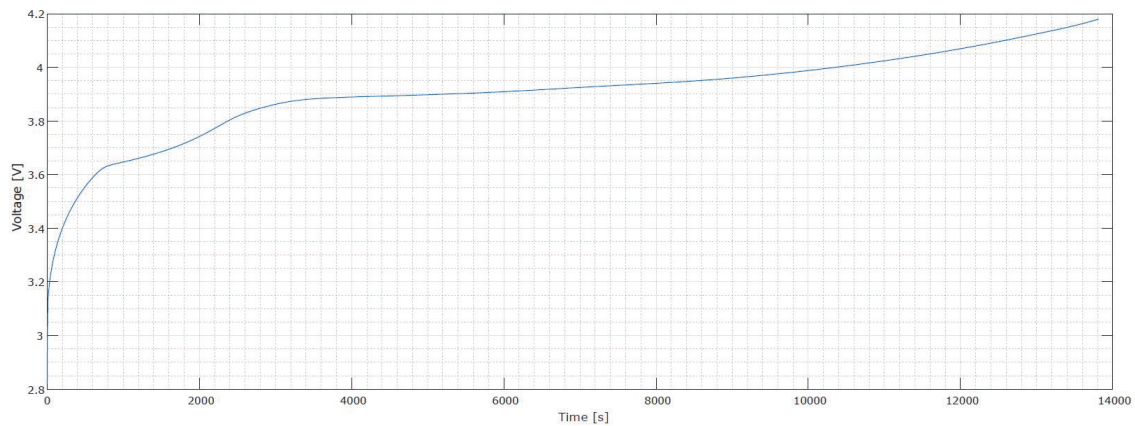
Figure 9. LI-ION battery charge characteristic curve for 4 channels. Source [8].
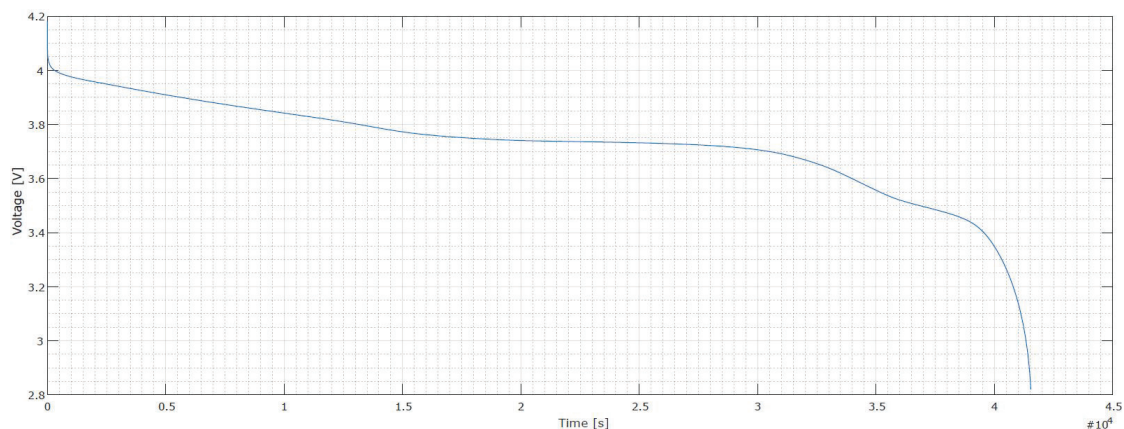
Figure 10. LI-ION battery discharge characteristic curve for 4 channels. Source [8].

The charge and discharge curve for the LI-ION battery in figures 9 and 10, together with the results in table 5, show that output voltage varies in time and that it depends on the charge connected to it. However, the Boost and Inverter topologies maintain constant input voltage over time for the LDOs. As a result, the output voltage of the power management system is constant despite the variation in battery voltage.

Results of noise characterization and reduction

At the beginning of this project, PSD analysis showed a spectral component at 50 Hz in all channels. This component corresponds to the power line, which is a common source of external noise. Figure 11 shows the power spectral density for channel 1, clearly evidencing a peak at 50 Hz with 50×10^{-2} V²/*Hz* magnitude.
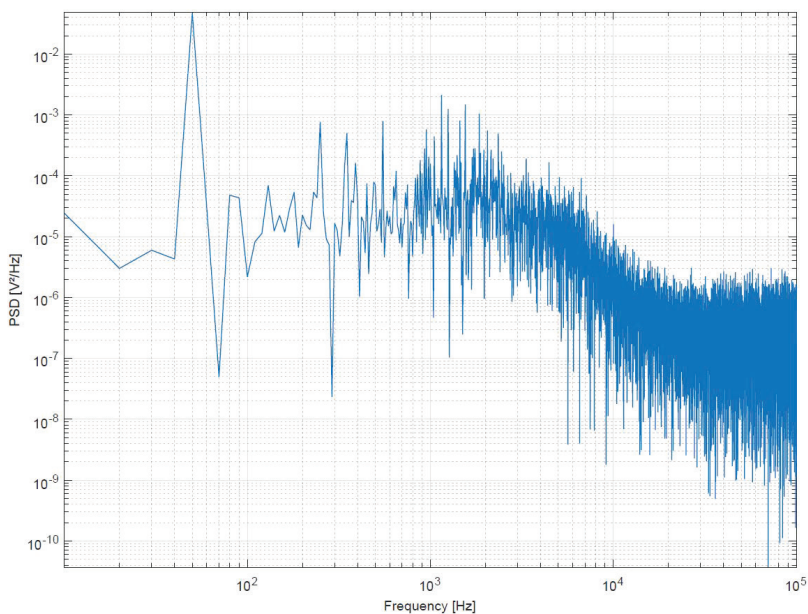
Figure 11. Power spectral density for channel 1. Source [8].

Coupling a printed sensor to the analog system increased the noise added by the power line. The reason behind this phenomenon is the antenna-like behavior by the sensor, thus capturing external electromagnetic noise. Therefore, an aluminum case was used to have an appropriate shield against external noise sources, and thus, reduce the effects of the power line and the antenna-like behavior by the sensor.

Figure 12. Modified aluminum case to contain analog system. Source [8].

Figure 13 shows the power spectral density of channel 1 when the analog system is introduced in the aluminum case. As can be seen, the 50 Hz spectral component has been successfully reduced. In the case of figure 13, the 50 Hz magnitude is now 3×10^{-6} $V^2/Hz.$ The same behavior was observed in all the other channels.
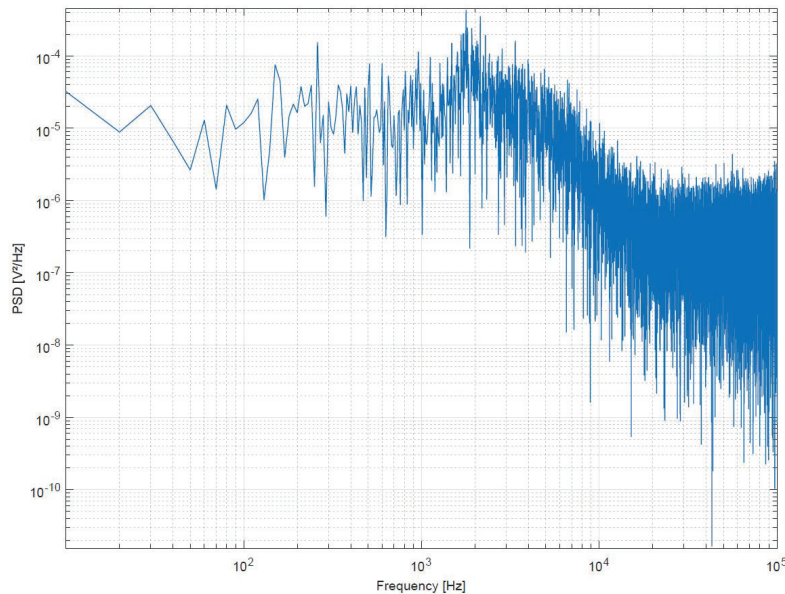
Figure 13. Power spectral density of channel 1 with the analog system
inside the aluminum case as a shield. Source [8].

Tables 6 and 7 show noise characterization results after introducing the analog system to the aluminum case shown in figure 12. Each row represents a channel in order to compare the noise level depending on the feedback resistor position. Additionally, each table shows RMS value and peak-to-peak voltage results. In these experiments, silver nanoparticles were not used on the printed sensor, since the purpose was to evaluate only system noise in the absence of an input signal.

Table 6. Noise characterization in each channel of the analog system when there
is not a printed sensor coupled to the circuit input. Source: [8].

Channel	RMS (mV)	Peak-to-peak voltage (mV)
1	0.209	1.849
2	0.196	1.817
4	0.199	1.640

Table 7. Characterization of noise in each channel of the analogue system when
there is a printed sensor coupled to the circuit input. Source: [8].

Channel	RMS (mV)	Peak-to-peak voltage (mV)
1	0.210	1.705
2	0.196	1.962
4	0.198	1.624

In the absence of an input signal, tables 6 and 7 show that there are no significant differences in terms of noise addition as a result of the positioning of feedback resistors. The difference in RMS values and peak-to-peak voltage is negligible between each channel. Furthermore, shielding has reduced the noise added by the printed sensor, due to its antenna-like behavior. This is evident when comparing tables 6 and 7, which present minimal differences between their peak-to-peak and RMS values.

Noise comparison in power sources

Table 8 and 9 present the noise characterization for the three power rails used from both, the TENMA72-10495 desktop power supply and the designed power management system. Because the desktop source transforms AC into DC, the noise level is considerably higher than the LI-ION battery. In addition, LDOs reduce the noise produced by the Boost and Inverter switching sources. As a result, the power management system improves device sensitivity.

Table 8. RMS and peak-to-peak measurement of the noise in the TENMA72-10495 power supply. Source: [8].

Output voltage	RMS (mV)	Peak-to-peak voltage (mV)
3.3	1.747	28.744
5	1.648	29.146
-5	2.581	44.221

Table 9. RMS and peak-to-peak measurement of the noise in the power management system. Source: [8].

Output voltage	RMS (mV)	Peak-to-peak voltage (mV)
3.3	0.353	2.894
5	0.367	3.698
-5	0.186	2.332

Quantification of noise due to electrolyte

Table 10 shows the noise characterization of the electrode-electrolyte interface for each channel. Obtaining these values was possible only after shielding the circuit with the aluminum case, since the noise caused by the power line was superimposed on any other signal, interfering with the analysis.

Table 10. Noise added by the electrode-electrolyte interface on each available channel. Source: [8].

Channel	RMS (mV)	Peak-to-peak voltage (mV)
1	5.300	31.357
2	4.701	33.568
4	2.942	19.698

Frequency response

Table 11 includes cutoff frequency for each channel. Only channel 1 approaches the design criteria of the low-pass filter. A possible cause for the cutoff frequency breach in channels 2 and 4 is the degradation of some electronic components due to extensive circuit use in several tests over the last year. However, the cutoff frequency of all channels is in the order of KHz range, sufficient for the detection of silver nanoparticles.

Table 11. Cutoff frequency for each channel of the analog circuit. Source: [8].

Channel	Cutoff frequency (KHz)
1	3.2
2	2.0
4	2.4

Conclusions and / or recommendations

A power system meeting the power requirements of the silver nanoparticle sensor was designed and implemented. Moreover, this design is light enough to allow easy sensor transport. The operating time of the device is 11 hours and 30 minutes when using four channels. Furthermore, it allows increasing the number of channels to 60, with an operating time of 3 hours and 45 minutes. The new power source is more noise-free than the TENMA72-10495 source, thus improving silver nanoparticles detection.

External noise sources were identified and effectively reduced with the use of an aluminum shield. This shield also counteracts the antenna-like behavior of the printed sensor. Additionally, the aluminum case helped to quantify noise derived from the electrode-electrolyte interface. This also means that there is now a better scenario for future device testing.

Detecting silver nanoparticles can be satisfactorily made with the current cutoff frequency of the low-pass filters, since it is in the range of KHz. However, in a future system update, it is expected that all filters will meet the design criteria.

Noise characterization was made using printed sensors of different lengths. It was observed that by increasing length, added noise increased too. The longer the length, the printed sensor is more sensitive to small openings in the aluminum shield and to vibrations on the surface. Furthermore, the coupling between the input of the analog circuit and the printed sensor leaves room for oscillations between metal contacts. The effect of these oscillations is greater for longer sensors. Using short printed sensors and improving coupling with the analog circuit is recommended for future updates.

The design of the power management system can be implemented without LDOs at the expense of increasing system noise. However, this change in the end device may be considered if the extra noise does not affect the detection of silver nanoparticles. As a result, manufacturing costs would be reduced, since both LDOs and associated electronic components would not be used anymore.

Because this is an ongoing project, there are numerous assessments and improvements to be made. For example, unifying all systems (power management system, digital system and analog system) in a single PCB, increasing the number of channels, detecting silver nanoparticles, among others. However, the advances made in this project bring us closer to the creation of a portable device for the detection of silver nanoparticles in-situ.

Acknowledgment

References

[1] K. Chitra and G. Annadurai. "Antibacterial activity of pH-dependent biosynthesized silver nanoparticles against clinical pathogen," BioMed Research International, vol. 6, 2014. URL https://doi.org/10.1155/2014/725165

[2] K. J. Krause, A. Yakushenko and B. Wolfrum. "Stochastic on-chip detection of subpicomolar concentrations of silver nanoparticles," Analytical Chemistry, vol. 87, pp. 7321–7325, 2015. URL https://doi.org/10.1021/acs.analchem.5b01478. PMID: 26079741.

[3] F. Sambale et al. "Investigations of the toxic effect of silver nanoparticles on mammalian cell lines," Hindawi, vol. 2015, 2015. URL https://doi.org/10.1155/2015/136765

[4] A. Mohammadi Bardbori, M. Korani, E. Ghazizadeh, S. Korani, and Z. Hami. "Effects of silver nanoparticles on human health," European Journal of Nanomedicine, vol. 7, pp. 51–62, 2015. URL https://doi.org/10.1515/ejnm-2014-0032

[5] S. V. Sokolov, S. Eloul, E. Kätelhön, C. Batchelor-McAuley and R. G. Compton. "Electrode-particle impacts: a user's guide," Phys. Chem. Chem. Phys, vol. 19, pp. 28–43, 2017. URL http://dx.doi.org/10.1039/C6CP07788A.

[6] J. Rapp. Compact sensitive Amplifier Circuit for the Detection of Nanoparticles Design und Evaluation einer Verstärkerschaltung für die Kon- zentrationsmessung von Nanopartikel. Bachelor thesis, 2017.

[7] D. W. Kumsa et al. "Electron transfer processes occurring on platinum neural stimulating electrodes: a tutorial on the i(Ve) profile," Journal of Neural Engineering, vol. 13, 2016. URL http://stacks.iop.org/1741-2552/13/i=5/a=052001

[8] O. Soto. Optimization of an analogue circuit design for a portable nanoparticle detection device (POND) using printed sensors, graduation project to obtain the Bachelor's Degree in Electronics Engineering, Costa Rica Institute of Technology, Cartago 2018. URL https://repositoriotec.tec.ac.cr/handle/2238/10407

[9] P. G. Figueiredo, L. Grob, P. Rinklin, K. J. Krause and B. Wolfrum. "On-chip stochastic detection of silver nanoparticles without a reference electrode," ACS Sensors, vol. 3, pp. 93–9, 2018. URL https://doi.org/10.1021/acssensors.7b00559. PMID: 29276833.

[10] L. Grob. Design and Implementation of a Miniaturised Bipotentiostat in Master thesis, 2015.

[11] T. H. Shuang and R. G. Compton. "Nano-impacts: An electrochemical technique for nanoparticle sizing in optically opaque solutions," ChemistryOpen, vol. 4, pp. 261–263, 2015. URL https://onlinelibrary.wiley.com/doi/abs/10.1002/open.201402161

[12] K. Kanokkanchana, E. N. Saw and K. Tschulik. "Nano-impact electrochemistry: Effects of electronic filtering on peak height, duration, and area," ChemElectroChem, vol. 5, 2018. URL https://doi.org/10.1002/celc.201800738

[13] R. Mancini. Op Amps for Everyone Design Reference, 2001.

[14] K. Armstrong, Testing Conducted Emissions, pp. 1–20, 2002.

[15] Gamry Instruments. The Faraday Cage: What Is It? How Does It Work?, pp. 1–3, 2010.

[16] A. Kumar and P. Madaan. Top 10 EMC Design Considerations. Cypress Semiconductor 4, 2011.

[17] F. Hussien and B. Eckmann. Guide to Choosing the Best DCDC Converter for Your Application, 2016.

[18] R. V. Roy. Power Management Introduction, pp. 1–11, 2014.

[19] Texas Instruments. Understanding Boost Power Stages in Switchmode Power Supplies: Application Report, 1999.

[20] Texas Instruments. Understanding Buck Power Stages in Switchmode Power Supplies: Application Report, 1999.

[21] S. Valavan. Understanding electromagnetic compliance tests in digital isolators.

[22] M. Day. Understanding Low Drop Out (LDO) Regulators, 2002.

[23] K. V. Renterghem. How to measure LDO noise, 2015.

[24] Keysight Technologies. Spectrum Analysis Basics, pp. 1–89.

[25] J. C. Teel. Understanding noise in linear regulators, pp. 5–8, 2005.

[26] A. Kay. Operational Amplifier Noise: Techniques and Tips for Analyzing and Reducing Noise, (january 2012), first edn.

[27] A. Pini. Analyze noise with time, frequency, and statistics, 2017.[28]

[27] S. W. Smith. Statistics, "Probability and Noise. In technical Publishin", in The Scientist and Engineer's Guide to Digital Signal Processing Statistics, Probability and Noise, chap. 2, 664. San Diego, California, 1999.